Nanostructure Synthesis

Synthesis of Ultrathin Zinc Nanowires and Nanotubes by Vapor Transport**

*Xiaogang Wen, Yueping Fang, and Shihe Yang**

One of the most important challenges in the synthesis of nanowire materials is the control of size and morphology.[1,2] With regards to metallic nanowires, most studies have so far concentrated on gold and silver nanowires,[3–6] while less has been reported about their zinc counterparts. Ultrathin zinc wires are expected to display intriguing properties, such as metal–insulator transitions and 1D superconductivity. The magnetoresistance and thermopower of zinc-nanowire composites in insulating matrices were studied by Wu and coworkers,[7] who found that zinc nanowires with a diameter of 15 nm are metallic, whereas smaller nanowires show weak 1D localization with resistivity proportional to $T^{-1/2}$. The thermopower of zinc nanowires with a diameter of 4 nm was found to saturate at −130 μV/K. However, the structural details of the embedded zinc nanowires have not been investigated. Zinc nanowires may also be a good template to form 1D nanostructures of other important materials, such as ZnO, ZnS, and Cu.[8,9] Zinc nanowires and nanotubes with core/shell structures of Zn/ZnO and Zn/ZnS were usually prepared from ZnO[10–12] or ZnS[13–15] as precursors by a vapor–solid (VS) process. Recently, Peng et al. reported the synthesis of zinc nanofibers with diameters of 50–200 nm by evaporation of pure zinc powders.[16] Also, zinc nanowires have been prepared by electrochemical etching in HF solution.[17] Until now, however, the synthesis of discrete, ultrathin (< 10 nm) zinc nanowires and nanotubes had not been reported, although 6-nm-wide ZnO nanobelts have been described recently.[18] Herein, and to the best of our knowledge, we report the first synthesis of discrete zinc nanowires and nanotubes, with diameters of several nanometers, by a VS process using zinc foil as the precursor. The key to our success is the use of H_2O and NH_3 as molecular directing agents.

To synthesize zinc nanowires, the evaporation temperature was fixed at 900 °C, as lower temperatures (below 750 °C) failed to yield any zinc-based products. Figure 1 a shows an X-ray diffraction (XRD) pattern of as-prepared zinc nanowires. All of the observed signals for the sample match very well with those of hexagonal zinc ($a = 2.665$, $c = 4.947$ Å,

[*] X. Wen, Dr. Y. Fang, Prof. S. Yang
Department of Chemistry
Institute of NanoScience and Technology
The Hong Kong University of Science and Technology
Clear Water Bay, Kowloon, Hong Kong (China)
Fax: (+852) 2358-1594
E-mail: chsyang@ust.hk

[**] We are grateful to the Research Grant Council of Hong Kong and the Chemistry Department of the Hong Kong University of Science and Technology for supporting this research. S.Y. thanks the Hong Kong Young Scholar Cooperation Research Foundation of NSFC.

Supporting information for this article is available on the WWW under http://www.angewandte.org or from the author.

  DOI: 10.1002/ange.200500438

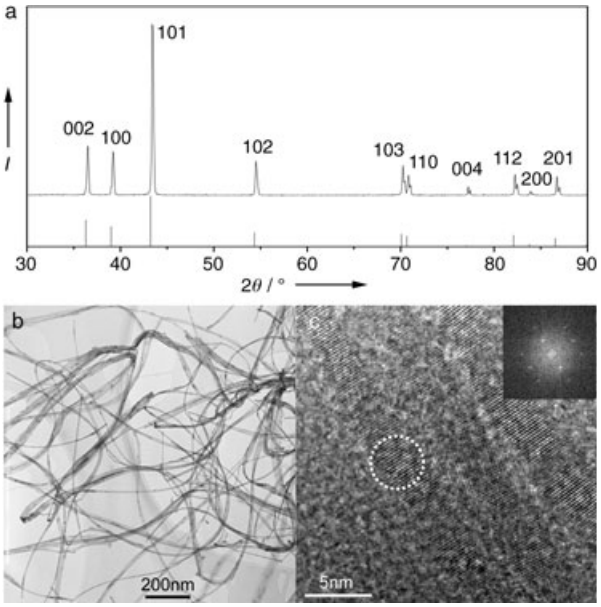

Figure 1. a) XRD pattern of the zinc nanowires prepared by the vapor-transport method, b) a typical TEM image of zinc nanowires prepared in an NH_3 atmosphere, and c) HRTEM image of three parallel zinc nanowires (the inset shows the corresponding FFT pattern of the sample indicated by the white dotted circle in the main panel). The zinc nanowires were deposited at 190–250 °C.

obtained from the JCPDS 04-0831 card), which indicates that the nanowires consist predominantly of pure zinc. Shown in Figure 1 b is a typical transmission electron microscopy (TEM) image of the zinc nanowires deposited over a temperature range of 190–250 °C, with a flow of N_2 of 20 sccm (standard cubic centimeters per minute) for carrying NH_3 (with a trace amount of residual water, $H_2O/NH_3 \approx 1{:}20$). The zinc nanowires have a uniform diameter of 3–8 nm (average diameter ≈ 5 nm) along its entire length, which is up to tens of micrometers. Some of the nanowires are bundled together. Figure 1 c shows a high-resolution TEM (HRTEM) image of three parallel zinc nanowires. The nanowires are 3–4 nm in diameter with excellent uniformity. Clear fringes perpendicular to the nanowire axis can be seen with an interplanar spacing of 0.25 nm in accordance with the distance between the (002) crystal planes, which suggests that the zinc nanowires grow along the [001] direction, that is, along the direction of the *c* axis of hexagonal zinc. This observation is also reflected in the fast Fourier transform (FFT) pattern (inset, Figure 1 c) of the area indicated by a white dotted circle in the main panel.

The products deposited in regions of different temperature of the furnace have different sizes and morphologies, as demonstrated by their TEM images (see the Supporting Information). The products formed in the 200 °C region are uniform, ultrathin nanowires with a diameter of 3–8 nm. In the 150 °C region, although thin nanowires of several nanometers in diameter can still be found, much thicker nanowires (50–70 nm) are found abundantly in a more twisted form. Finally, when the deposition temperature is 100 °C, the nanowires become even thicker (90–100 nm in diameter) and, moreover, these twisted nanowires are tangled together to form a network structure. Note that although the nanowires thicken as the deposition temperature decreases, they all have a pure hexagonal structure based on XRD and energy dispersive X-ray (EDX) analyses. Oxidized surface layers (ZnO) were not identified in these nanowires by HRTEM.

When the ammonia solution was replaced by pure water, ultrathin zinc nanotubes, rather than nanowires, were obtained as shown in Figure 2. In this experiment, the water

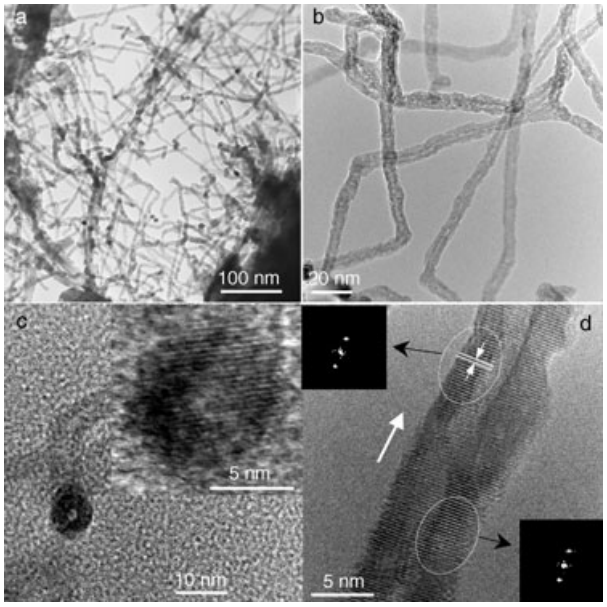

Figure 2. TEM images of zinc nanotubes synthesized in a water-vapor atmosphere. a) Low magnification, b) higher magnification, c) cross-sectional view of a tube end (the inset shows a HRTEM image), and d) HRTEM image of a single zinc nanotube (the insets show the FFT patterns from regions enclosed by the white dashed ellipsoids in the main panel).

vapor was transported into the reaction tube by N_2 through a sealed water bubble aeration setup. Figure 2 a is a low-magnification TEM image of the as-prepared zinc nanotubes, which have a uniform diameter (5–8 nm) along their length (several hundred nanometers to several micrometers) and are mostly open-ended. A higher magnification TEM image is shown in Figure 2 b and reveals the tubular structure more clearly. The inner diameters of the nanotubes are about 1–2 nm and the wall thicknesses are about 2–3 nm. The nanotubes are not very smooth on either the inner or outer surfaces. Although the 1D structure is generally tubelike, the zinc tubes are not completely continuous and the inner channels are often blocked. Figure 2 c highlights the end of a single nanotube so that the cross section can be seen directly. The nanotube appears to have a circular cross section; the diameter of the inner tube is 1.5 nm and the wall thickness is 3.0 nm. From the HRTEM image of the tip of the zinc nanotube in the inset of Figure 2 c, well-defined fringes with a spacing of approximately 0.27 nm can be seen and correspond to double the spacing between the (110) crystal planes ($d_{110} =$ 0.133 nm). Consequently, the cross-sectional plane of the nanotube is the *ab* plane of hexagonal zinc, which suggests

that the growth direction of the nanotube is [001], similar to that for the zinc nanowires. Figure 2d shows a higher magnification HRTEM image of a single zinc nanotube. The tubelike structure is seen more clearly, and fringes spaced by approximately 0.25 nm are found to lie perpendicular to the tube axis, which confirms the [001] growth direction of the nanotube. As can be seen from the inset of Figure 2d, the FFTs of both side walls (enclosed by white dotted ellipsoids in the main panel) display the same spotted pattern and indicate the same crystal structure with the length of the nanotube extending along the [001] direction.

When only pure N_2 was used as the carrier gas, zinc nanowires could not be obtained. Instead, most of the products were well-defined polyhedral microparticles and XRD data indicate that the products are still pure zinc (see the Supporting Information). The microparticles deposited on an aluminum-foil substrate have a uniform size of 3–5 μm. Higher magnification scanning electron microscopy (SEM) images indicate that the particles have faceted morphologies that range from hexagonal columns (major) to polyhedra (minor; see the Supporting Information).

For comparison, the vapor–liquid–solid (VLS) approach was also explored to synthesize zinc nanowires. A small piece of lead foil (placed in the high-temperature region together with the zinc foils) was chosen as a catalyst as it has an appropriate melting point (325 °C). N_2/NH_3 was used as the carrier gas, while the other conditions were kept the same. Indeed, zinc nanowires could also be produced by the VLS process as shown in Figure 3. Most of the nanowires are capped by a nanoparticle on their tips (see Figure 3a), as expected for the VLS process. The tips can be seen more clearly in Figure 3b. EDX analysis confirmed that the nanoparticles comprise lead and that the nanowires consist purely of zinc. Interestingly, the diameter of the zinc nanowires here (15–25 nm), although a little larger than the diameter of the nanowires prepared by the VS method, is much smaller than that of the lead nanoparticles (50–60 nm). The fact that thin zinc nanowires can also be formed on large lead nanodroplets by the VLS process is perhaps because of the confining effect of ammonia. In some cases, several zinc nanowires share a common, relatively large catalytic nanoparticle ($\approx$100 nm; Figure 3c), which suggests that this nanoparticle can provide nucleation sites for the growth of several nanowires simultaneously. The zinc nanowires prepared by the VLS method are obtained in a higher yield than those prepared without the lead catalyst, but they are less uniform and have a larger diameter probably as a result of the non-uniform and large sizes of the lead nanoparticles.

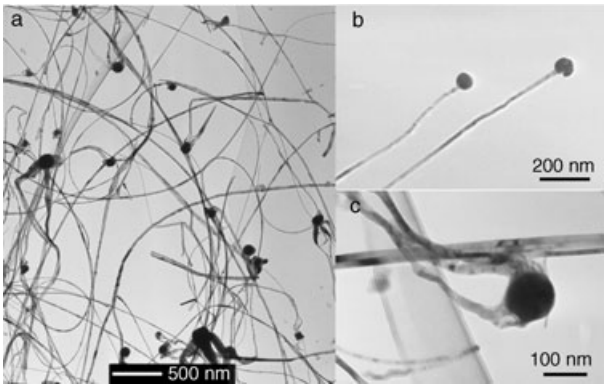

Figure 3. Zinc nanowires prepared by the VLS process. a) A typical TEM image, b) at higher magnification, and c) at even higher magnification to show that several zinc nanowires grow from one catalytic lead nanoparticle.

Presumably, the formation of the zinc nanowires in the absence of a catalyst is through a vapor–solid (VS) process. The zinc precursor was evaporated at high temperature (900 °C), and the vapor was transferred to the deposition region (200 °C) by carrier gas. On the basis of the data presented above, the size and morphology of the products are mainly controlled by the temperature of evaporation and deposition, and the composition of the carrier gas. A higher evaporation temperature ensures the formation of a sufficient density of zinc atoms or clusters for nucleation as well as a large temperature gradient favorable for the growth of zinc nanowires. At higher deposition temperatures the growth is relatively slow, whereas at lower temperatures the growth is faster. These temperature effects, when considered together with appropriate compositions of carrier gas, can be exploited so that ultrathin nanowires can be synthesized at high temperatures and thicker nanowires at low temperatures.

Here, the carrier gas appears to be the most important factor and is, in fact, essential to controlling the synthesis of the nanowires. The coordination of NH_3 and H_2O molecules to zinc atoms and clusters at the temperature region in which the nanowire deposition occurs plays a particularly important role. In this way, they act as capping agents to promote anisotropic growth of the nanowires. Specifically, the preferential adsorption of NH_3 and H_2O on the surfaces of the zinc nanowire, other than at the tips, has the effect of restraining the radial, but not the axial, growth so that 1D growth is facilitated. It is not surprising that such a molecularly directed growth yields nanowires that are much thinner than those from the VLS process. For the synthesis of zinc nanotubes in a water-vapor atmosphere, water clusters form much more easily through hydrogen-bonding interactions than ammonia clusters in the deposition region and so may act as templates for the nucleation of zinc. Such a zinc-shell structure that is supported by a core of water clusters may eventually evolve into a tubelike structure with open ends as a result of morphological developments of the water-cluster template (Scheme 1). The soft and dynamic nature of the water-cluster

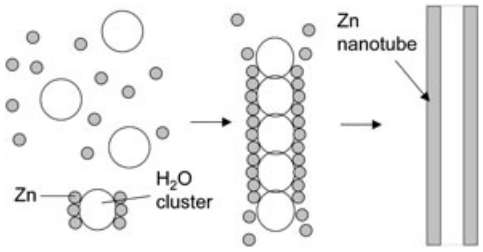

Scheme 1. A schematic representation of a possible mechanism for the formation of zinc nanotubes in the presence of water vapor.

template may explain the observed imperfect structure of the zinc nanotubes. A clearer understanding of the growth mechanisms of the nanowires and nanotubes requires more-detailed studies.

In summary, ultrathin zinc nanowires and nanotubes have been synthesized by both VS and VLS processes with pure zinc. The composition of the carrier gas is the key to controlling the size and morphology of the nanoproducts. Zinc nanowire crystals with diameters as small as 3 nm (average diameter $\approx$ 5 nm) could be synthesized in an ammonia atmosphere. Furthermore, when water vapor was used instead of ammonia, zinc nanotubes were obtained that are characterized by an inner diameter of 1–2 nm and a wall thickness of 2–3 nm. Our study highlights the essential role of small polar molecules, the adsorption of which modifies the kinetics of crystal growth and thus directs the 1D growth of zinc. Ultrathin metallic nanowires and nanotubes, with sizes that approach the Fermi wavelength, offer new opportunities to explore the effects of size on the transport and photonic properties of these materials and promise a wide range of applications in nanotechnology.

Experimental Section

The experimental setup consisted of a horizontal tube furnace (120 × 10 cm), a quartz tube (100 × 5 cm), and a gas-flow control system. Zinc foils (10 × 10 × 0.1 mm^3; 99.9% purity, Aldrich) were washed with absolute ethanol twice before loading onto a quartz substrate, which was positioned at the end of the quartz tube. A piece of aluminum foil or a quartz slide was positioned at the opening end of the quartz tube to serve as a product deposition substrate. The quartz tube was then mounted in the middle of the tube furnace. A flow of high-purity nitrogen (> 99.995%) was introduced into the quartz tube through a sealed container containing a diluted aqueous solution of ammonia (6.0 M) or pure water at a fast rate (about 200 sccm) for 40 min to remove air from the system. Afterwards, the N_2 flow was adjusted to 20 sccm and the tube furnace was heated to 900 °C at a rate of 30 °C min^{-1}. After heating at this temperature for 5 h, the system was allowed to cool unaided to room temperature and black products were obtained. XRD analyses were carried out on a Philips PW 1830 X-ray diffractometer with a 1.5405-Å $Cu_{K\alpha}$ rotating anode point source operated at 40 kV and 40 mA. Kβ radiation was eliminated with a nickel filter. TEM measurements were performed on Philips CM20 and JEOL 2010F transmission electron microscopes with an accelerating voltage of 200 kV. SEM images were observed with a JEOL 6300F microscope at an accelerating voltage of 15 kV.

Received: February 5, 2005
Published online: May 4, 2005

Keywords: high-temperature chemistry · nanostructures · synthesis design · zinc

[1] X. F. Duan, C. M. Lieber, *Adv. Mater.* **2000**, *12*, 298.
[2] Z. L. Wang, *Nanowires and Nanobelts: Materials, Properties, and Devices*, Kluwer Academic/Plenum Publishers, Boston, **2003**.
[3] Y. G. Sun, B. Gates, B. Mayers, Y. N. Xia, *Nano Lett.* **2003**, *3*, 955.
[4] X. Y. Zhang, L. D. Zhang, Y. Lei, L. X. Zhao, Y. Q. Mao, *J. Mater. Chem.* **2001**, *11*, 1732.
[5] J. K. N. Mbindyo, B. D. Reiss, B. R. Martin, C. D. Keating, M. J. Natan, T. E. Mallouk, *Adv. Mater.* **2001**, *13*, 249.
[6] B. H. Hong, S. C. Bae, C. W. Lee, S. Jeong, K. S. Kim, *Science* **2001**, *294*, 348.
[7] J. P. Heremans, C. M. Thrush, D. T. Morelli, M. C. Wu, *Phys. Rev. Lett.* **2003**, *91*, 076804.
[8] Q. Li, C. R. Wang, *Chem. Phys. Lett.* **2003**, *375*, 525.
[9] Q. Li, K. W. Kwong, D. Ozkaya, D. J. H. Cockayne, *Phys. Rev. Lett.* **2004**, *92*, 186102.
[10] Y. F. Yan, P. Liu, M. J. Romero, M. M. Al-Jassim, *J. Appl. Phys.* **2003**, *93*, 4807.
[11] X. Y. Kong, Y. Ding, Z. L. Wang, *J. Phys. Chem. B* **2004**, *108*, 570.
[12] J. Y. Li, X. L. Chen, *Solid State Commun.* **2004**, *131*, 769.
[13] Y. W. Wang, L. D. Zhang, G. W. Meng, C. H. Liang, G. Z. Wang, S. H. Sun, *Chem. Commun.* **2001**, 2632.
[14] Y. C. Zhu, Y. Bando, Y. Uemura, *Chem. Commun.* **2003**, 836.
[15] J. Q. Hu, Q. Li, X. M. Meng, C. S. Lee, S. T. Lee, *Chem. Mater.* **2003**, *15*, 305.
[16] X. S. Peng, L. D. Zhang, G. W. Meng, X. Y. Yuan, Y. Lin, Y. T. Tian, *J. Phys. D* **2003**, *36*, L35.
[17] S. S. Chang, S. O. Yoon, H. J. Park, A. Sakai, *Mater. Lett.* **2002**, *53*, 432.
[18] X. D. Wang, Y. Ding, C. J. Summers, Z. L. Wang, *J. Phys. Chem. B* **2004**, *108*, 8773.

